Influence of High Temperature Heat Treatment on in situ Transformation of Mo-rich Eutectic Carbides in HSS and Semi-HSS Grades

J. Tchoufang Tchuindjang[1,a], Mario Sinnaeve[2,b] and J. Lecomte-Beckers[1,c]
[1] MMS Unit, Aerospace and Mechanics Dpt., University of Liège
Chemin des Chevreuils 1 – 4000 Liège, Belgium
[2] Marichal Ketin – Verte voie 39 – 4000 Liège, Belgium
[a]j.tchuindjang@ulg.ac.be, [b]rolls@mkb.be, [c]jacqueline.lecomte@ulg.ac.be

Keywords: *HSS, Solidification sequence, eutectic carbides, solid state transformations, DTA, TC*

Abstract. Alloys of the complex system Fe-Cr-C-X, where X is a strong carbide forming-element are well known to exhibit interesting mechanical properties, including wear and abrasion resistances. Such a tribological behavior is mainly due to the presence of carbides especially those obtained during the solidification route and that are known as primary or eutectic carbides. It may therefore be interesting to determine the relative stability of primary carbides when considering thermal and thermomechanical treatments performed at a temperature high enough to allow either the homogenization of the matrix or the occurrence of a desired grain size. This thermal stage is often required to produce tailored microstructures that can lead to improved mechanical properties. In this work a series of thermal treatments performed on samples originated from cast foundry parts were done. Raw materials are both HSS and semi-HSS grades used in application where wear resistance is needed. Thermo-Calc® (TC) simulations and Differential Thermal Analysis (DTA) were performed to determine the crystallization behavior and the subsequent solid state transformations of the studied alloys respectively in equilibrium and in non equilibrium conditions. Light and Scanning Electron Microscopies were done together with hardness measurements in order to enhance metallurgical features of the heat treated samples. Image analysis yielded the determination of carbides volume fractions. It appears from microstructural analyses and carbides quantification that Mo-rich eutectic carbides undergo in situ phase transformations during heat treatments. In fact Mo-rich M_2C carbides transform themselves into MC, M_6C and C-rich carbide, through a so-called "budding" phenomenon. Such a phenomenon is the evidence of a preferential migration of some atoms that escape from the parent M_2C carbide to diffuse further away from their initial site with increasing time and temperature. The stable or metastable nature of eutectic carbides is also discussed from DTA and TC results, as M_2C carbides found in both as-conditions and DTA samples were not predicted by equilibrium conditions.

Introduction

HSS standing for High Speed Steels are high alloyed steels belonging to the complex system Fe-Cr-C-X, where X is a strong carbide forming-element such as Mo, V or W. HSS grades are widely used as work rolls for Hot Strip Mill (HSM) where carbides content promote enhanced mechanical properties together with wear and oxidation resistances [1-7].
Carbides can be of three types, namely the primary carbides, the eutectic carbides, and the secondary carbides [1-6, 8-13].
Primary and eutectic carbides are formed during solidification, whereas secondary carbides precipitate in the solid state, below the solidification range. Secondary carbides are fine

precipitates appearing either as a result of solid state phase transformations of delta-eutectoid or eutectoid type latter in the cooling stage of the casting route [9, 14], or during thermal treatment at temperature below or above austenitizing [2, 9, 15].
Primary carbides have got a size larger than that of eutectic ones, and their shape is quite similar to their crystallographic network as they precipitate directly from the liquid with a coarsening free behavior [1-6, 8-13].
The presence of an associated austenite phase within the eutectic carbides colonies influences both their morphology and size, especially as theses carbides appear at the end of the solidification process in a retained liquid located in the interdendritic areas that are limited in volume [1-6, 8-12].
The nature and composition of solidification carbides depend on both the chemical composition of the defined alloy and the cooling rate during the casting route, the latter parameter playing a very important role in the stable or metastable behavior of the carbide [2-6, 9-12, 16]. Low cooling rates will thus promote formation of stable carbides [16], as it is the case for the two types of Mo-rich carbide known as M_2C and M_6C, the former precipitating with higher cooling rates whereas the latter appearing with cooling rates as low as those obtained under equilibrium conditions [17].
In addition, the solidification process carried out with a certain cooling rate involved the occurrence of an undercooling phenomenon which is given by ΔT, the difference between the expected phase transformation temperature from the equilibrium conditions (i.e. by considering at any time and at any point of the liquid a possible diffusion of all the alloying elements) and the actual temperature of the same phase transformation in the non equilibrium conditions [3, 9, 12, 16]. The higher ΔT is, the higher the rate for carbides germs formation will be. Thus ΔT could influence the size, the morphology, the amount of eutectic carbides and the dendritism, as high values of ΔT promote both germination and formation of finer carbides [3, 6, 9, 12, 16, 18]. Furthermore ΔT can either shift the interval of a phase transformation or completely inhibit the reaction [3, 6, 9, 18].
Subsequent thermal treatments performed after casting route aim at producing a more homogeneous material without chemical heterogeneities such as micro segregations inherited from the casting. Heat treatments can help to destabilize unexpected phases by dissolving elements which constitute them in order to yield a homogeneous and tailored microstructure with improved properties, including a refined grain size and a high hardness for applications where wear resistance is needed [2, 7, 9].
In the equilibrium conditions, the transformation points are the same in both the heating and the cooling stages, contrary to non equilibrium conditions where a shift exists between transformations points in the heating mode and the corresponding ones during the cooling mode. The offset is often in the same direction compared to equilibrium conditions, which is a shift to lower temperatures during the cooling stage and shift to temperatures above those of thermodynamic equilibrium during heating. The temperature shift also depends on the heating or the cooling rates [3, 6, 9, 18].
However it could be possible to transform a metastable phase at a temperature below the dissolution point obtained from both equilibrium and non equilibrium conditions. This is the case for some carbides such Cr-rich M_7C_3 or M_3C [19-21], or Mo-rich M_2C carbides. Indeed several studies reported possible transformations of M_2C carbides under the effect of temperature into various secondary carbides such as MC + M_6C [12, 17], M_7C_3 + M_6C [13, 19], or even $M_{23}C_6$ + M_6C [19]. Step-by-step transformations of M_2C are also mentioned in the literature, including a first transformation in M_7C_3 carbide, followed by a destabilization of the M_7C_3 to form $M_{23}C_6$ or M_6C carbides [22, 23].

Most of the works dealing with these transformations of M_2C carbides focused on the nature of the newly formed products without necessarily describe the mechanism that supports M_2C decomposition [12, 13, 17, 19-23]. Furthermore the phase transformations occurring during thermal treatments carried out on alloys containing M_2C carbides in the previous works highlighted either the nature of the very fine secondary carbide precipitation during tempering [24, 25], or the coarsening of pre-existing carbides at higher austenitized temperatures [17, 18]. Whenever the complete decomposition of M_2C carbides is mentioned, the stability of the newly precipitated carbides is seldom issued [19].
The purpose of this study is to highlight the mechanism of M_2C in situ transformation at elevated temperature, with a focus on the chromium content of the surrounding matrix as it could be the driving force for such a transformation.

Materials and methods

The studied materials are respectively alloys of HSS type (A), semi-HSS type (Z) and High Chromium Steel (G). Cylindrical samples (∅10 mm, 10 mm thick) were collected from bars (2 kg weight) that have been cut out on the shell material of compound rolls obtained by a vertical spin casting process. Heat treatments were carried out on the bars. The studied zone is located 10 mm in depth within the shell material either for metallographic analyses or for DTA tests. Alloy A came from work roll used in the earlier finishing stands of a HSM, while G and Z grades were cut out of work rolls for roughing stands of HSM.
Average chemical compositions of the 3 studied alloys together with the rough dimensions of the as-cast work rolls are given in Table 1.

Table 1: Average chemical compositions (-wt%) of studied alloys and sizes of the rough as-cast rolls

	Alloying elements								As-cast Roll sizes (mm)
Grades	C	Si	Mn	Ni	Cr	Mo	V, Nb	Fe	
A	1.5-2.0	0.2-1.0	0.6-1.0	0.5-1.5	2.0-6.0	5.0-8.0	3.0-7.0	Bal.	∅800
G	1.0-1.5				10.0-14.0	3.0-6.0	<0.5		∅1200
Z	0.5-1.0				6.0-10.0	2.0-5.0	1.0-3.0		

Microstructures in the industrial as-cast conditions are showed in Figure 1. For the three studied grades, the microstructure in the as-cast conditions consists in a more or less continuous network of eutectic carbides located at grain boundaries with a matrix composed of martensite, bainite, retained austenite and possible softer phases such as pearlite. The unexpected occurrence of pearlite in such highly alloyed materials had been highlighted in a previous study [26]. The pearlite found in both A and G grades looks very fine and almost nodular, and it is sometimes called "troostite", which morphology is different from the conventional pearlite found in the Z grade.
ThermoCalc ® (TC) software was used to simulate the solidification in equilibrium conditions while considering Scheil-Gulliver (SG) model, where fast diffusion in the solid state of the most active element such as carbon, is assumed.
Non-equilibrium simulations were made using a NETZCH STA 449C apparatus, with a constant cooling rate of 5 °C/min. Differential Thermal Analysis (DTA) cycles involved heating until the complete melting of the sample (∅6mm-6mm height, cylinder), followed by a cooling sequence down to room temperature. The complete cycle is carried out with a permanent purge with argon. DTA tests helped determining non equilibrium phase

transformations, which were compared to those found with TC in the equilibrium conditions. DTA simulations also helped to set the temperature ranges for subsequent heat treatments done after casting. Temperatures were chosen in such a way that heat treatments occurred under austenitization and below critical carbides transformations points observed during the heating mode of DTA tests.

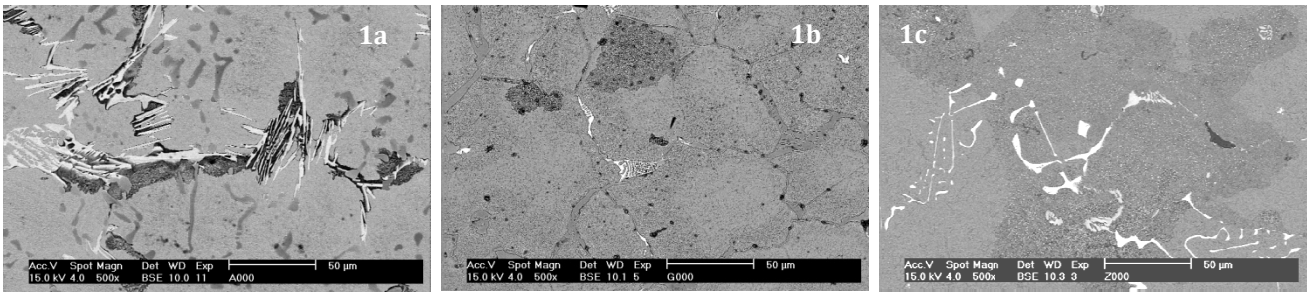

Figure 1: Microstructures of the studied alloys in the as-cast conditions (SEM images). ***1a*** *(Grade A, Nital etched): Network of globular MC (dark) and acicular M_2C (light) eutectic carbides in a matrix composed of martensite (MA) and retained austenite (RA), with some fine pearlite associated with M_2C;* ***1b*** *(Grade G, Nital etched): quasi-continuous network of M_7C_3 (grey) and M_2C (light) eutectic carbides at grain boundaries in a matrix composed of MA, RA, with some areas with fine pearlite (dark grey);* ***1c*** *(Grade Z, Nital etched): discontinuous network of MC (light, Chinese script Nb-rich) and M_2C (light, fine globular)eutectic carbides at grain boundaries in a matrix composed of MA, RA and pearlite in areas larger than those found on both A and G grades*

Heat treatments were done on bars in a BOUVIER TECHNOFOUR furnace equipped with a PID regulator and electrical resistances prior to calm air quenching. Table 2 illustrates the heat treatments carried out on each grade.

Table 2: Heat treatments performed on studied alloys (bars cut out of spun cast rolls)

Grades	Austenitizing Temperature (°C)	Holding time (min)	Quenching medium
A	1025, 1060, 1100	20, 60, 180	Calm air
G	980, 1025, 1060		
Z	1025, 1060, 1100		

Microstructure characterization was obtained through hardness assessment on the one hand, and by the means of optical and scanning electron microscopes on the other hand. Vickers bulk hardness measurements (HV 30) were carried out with a universal EMCO MC10 with an electronic cell force and a closed loop regulation. For each sample the average hardness value was obtained over 5 indentation points. Optical observations were made on a OLYMPUS BX60 microscope coupled with an OLYMPUS UC30 CCD digital camera, while SEM analyses were performed on a PHILIPPS XL 30 FEG-ESEM equipped with an Energy Dispersive X ray Spectrometer (EDS) detector.

The assessment of carbides volume fractions was made by quantitative metallography through image analysis with Image J® software while using pre-loaded plug-in for both segmentation and threshold [27]. For HSS A grade composed of massive eutectic carbides, optical images on the as-polished state were used for MC carbides assessment whereas coloring Groesbeck reagent was used for M_2C carbides. Carbides of G and Z grades were quantified using electron images, with an overall MC+ M_2C counting for Z grade, while only M_2C carbides were analyzed on G grade, leaving Cr-rich M_7C_3 carbides volume fraction unmeasured. The parameters used for image analysis are given in Table 3.

For HSS grade A, the carbides quantification from optical images respectively takes into account the edged effect (topographic) on MC carbides and the effect of refilling on M_2C carbides, to determine the upper bound of the average value. Two different algorithms

available in the in Image J plug-in, namely Li and Shandbag, were selected for approaching respectively the upper and the lower bounds either for MC and M_2C carbides. The secondary carbides present in the heat treated samples are not quantified as they were hardly distinguishable on optical images.
For grade G, a single algorithm is used in Image J (MaxEntropy), and then a filtering stage is done to remove very fine carbides which are isolated or associated with the M_7C_3. The upper limit of the M_2C is thus determined taking into account the secondary carbides present in the matrix, while the lower bound is determined with only eutectic M_2C carbides assessed without fine "secondary" carbides precipitated inside the grain.
For alloy Z, MC and M_2C carbides were measured in a single step and with a single algorithm in Image J (MaxEntropy). As for grade G, upper and lower bounds of the average volume fraction were obtained respectively with and without considering fine secondary carbides precipitated inside the grain.
For all the studied alloys, the final volume fractions of phases were obtained from the arithmetic average between upper and lower bounds.

Table 3: Parameters used for Image analysis on studied alloys (cylindrical polished sections, ∅10 mm)

Grades	Quantified carbides	Image origin	Image magnification	Single image resolution	Number of treated images	Sampled surface (%)
A	MC, M_2C	Optical	100x	2592x1944	20	6.4
G	M_2C	Electron		2048x1600		7.3
Z	MC +M_2C					

Results and observations

ThermoCalc (TC) simulations for solidification path in equilibrium conditions

TC simulations results are given in figure 2 which illustrates the solidification paths for the three studied grades while considering the SG model. Solidification curves allow determining both the nature (1st solid, possible peritectic reaction, eutectic carbides, etc.) and the amount of phases. In equilibrium conditions, MC, M_2C and M_7C_3 carbides are predicted for HSS A, M_7C_3 and M_6C for G grade and MC, M_6C, M_7C_3 and M_2C carbides for Z grade. The major phase transformations occurring during the solidification range are given in Table 4.

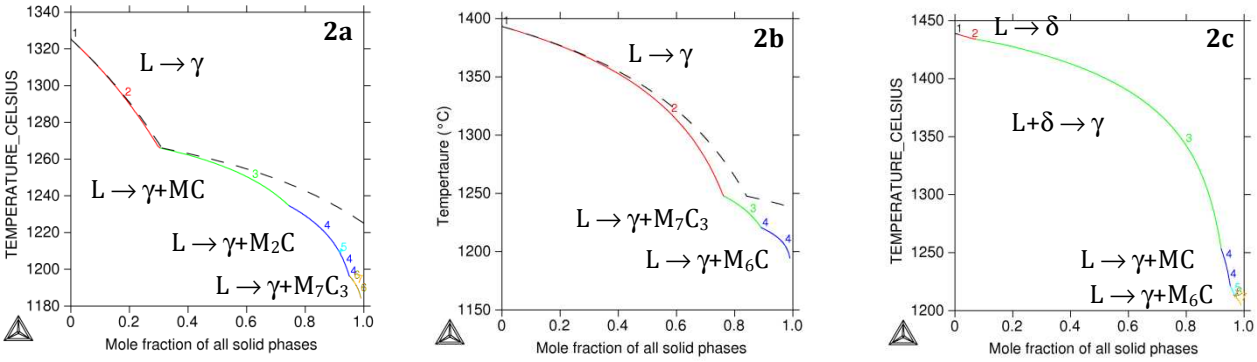

Figure 2: Solidification ranges for grades A (2a), grade G (2b) and grade Z (2c) as obtained from TC (SG Model) simulation with C as fast diffuser

DTA simulations for crystallization behavior in non-equilibrium and subsequent phase transformations, down to room temperature

The DTA curves for the cooling stages are given in figure 3. These curves illustrate the crystallization behavior of the three studied alloys in the non equilibrium conditions as the solidification range is between the liquidus and the solidus temperatures.
Table 4 gives the main results of DTA tests with the enhancement of phase transformations and related temperature ranges. The first solid to precipitate during the solidification range is δ-bcc for Z grade, and γ-fcc for both A and G grades. When δ is the first solid to precipitate, a new solid γ phase is formed later with decreasing temperature, towards a peritectic reaction involving the prior δ with the surrounding liquid. The remaining liquid located in the intercellular areas composed of γ dendrites undergoes eutectic transformations which lead to the precipitation of eutectic carbides, at the end of the solidification process [6, 9, 14]. But a discrepancy had been noticed during DTA tests on samples coming from A and G grades, as MC primary carbides appeared several times like the first solid for the former alloy while δ was sometimes the first solid to precipitate in G grade. Such discrepancies on the nature of the first solid could be linked to the undercooling effect as it has already been reported [3, 6, 9, 16, 18].
The number of the major phases that were formed during the solidification process could be determined from the observation of DTA curves, especially the peaks found on these curves as each one is related to a phase transformation. The possible phase transformations during the solidification of the studied alloys as suggested by DTA curves are given in Table 4, with an uncertainty remaining on the type (M_2C or M_6C) of the last eutectic carbide that precipitated on both G and Z grades.
The solidification range (SR) is given by the difference between the temperature at which the very first solid forms and the temperature at which the last drop of liquid is solidifies. SR was systematically found higher from DTA tests than the values predicted by TC simulations (160°C (DTA) # 100°C (TC) for A grade; 260°C#200°C for G and 290°C#250°C for Z).

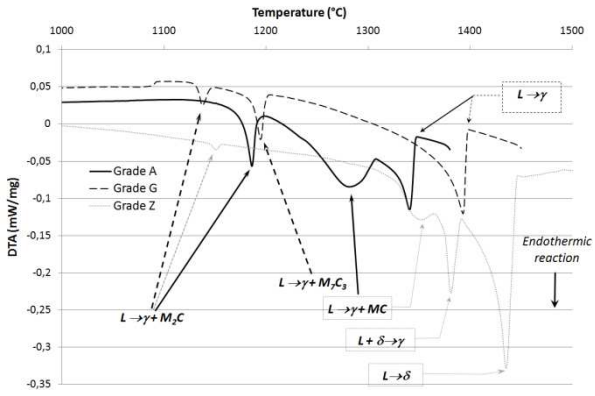

Figure 3: Crystallization behavior of grades A, G and Z from DTA tests (constant cooling rate of 5°C/min)

Table 4: Phase transformations and related temperature ranges in °C (DTA # TC)

Phase transformations	Grades	Temperature ranges (DTA)	Temperature ranges (TC)
L →δ	Z	**1443**-1433	***1440***-*1415*
L+δ→γ	Z	1393-1383	1415-1330
L→γ	A	**1345**-1340	***1325***-*1265*
	G	**1396**-1390	***1390***-*1245*
L→γ+MC	A	1305-1275	1265-1235
	Z	1366-1357	1330-1260
L→γ+M_7C_3	G	1201-1193	1235-1220
L→γ+M_2C (M_6C?)	A	1195-**1185**	*1235-**1230***
	G	1146-**1136**	—
	Z	1157-**1153**	*1200-**1190***
L→γ+M_6C	G	—	*1220-**1190***
	Z	—	1260-1200

Microstructural characterization, hardness

Typical microstructures obtained after heat treatments are illustrated in figure 4. A grade is composed of MC (V-rich) and M_2C (Mo-rich) carbides, G grade contains M_7C_3 (Cr-rich) and M_2C (Mo-Rich) carbides, whereas MC (Nb-rich Chinese script) and M_2C (Mo-rich) carbides are present in Z grade. There are two types of M_2C, the acicular or irregular one found in A grade (fig. 4a), and the lamellar or complex regular type found in both G and Z grades (fig. 4b, 4c) [6].
The effect of temperature and holding time on Mo-rich carbides stability is illustrated on fig. 5 (Grade A) and fig. 6 (Grade Z). For Grade A, an in situ transformation of Mo-rich M_2C carbide

was observed in most of the cases, which led to the precipitation of very fine carbides at the interface between the previous M_2C and the matrix (fig. 5c, d, e).

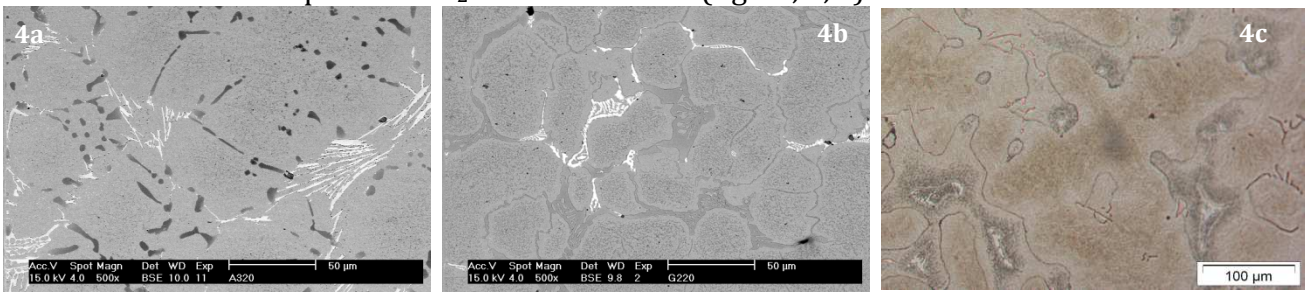

Figure 4: Typical microstructures of quenched specimens of the studied alloys, Back-Scattered Electron (BSE) images for 4a and 4b, and Optical image for 4c. ***4a*** *(Grade A, after 60' at 1060°C – 804HV): Intercellular eutectic carbides (V-rich MC (dark) and Mo-rich M2C (light) in a matrix composed of martensite (MA) with some retained austenite (RA);* ***4b*** *(Grade G, after 60' at 1025°C – 805HV): Quasi continuous network of eutectic carbides at grain boundaries (mainly Cr-rich M_7C_3 (dark grey) with some Mo-rich M_2C (light)) in a matrix composed of MA with some RA;* ***4c*** *(Grade Z, after 20' at 1060°C; Villella etched – 757HV): Intercellular eutectic carbides (Nb-rich MC (pink) and Mo-rich M_2C (light) surrounding by fully dispersed fine secondary carbides, in a matrix MA with some RA.*

The fine carbides formed at the interface are of two types, the first one being V-rich and the second one Mo-rich. Although the previous M_2C carbide kept its morphology unaltered, its chemical composition seemed to change as a decrease in V and Mo contents is observed together with an increase in Cr content (fig. 5c, d, e).

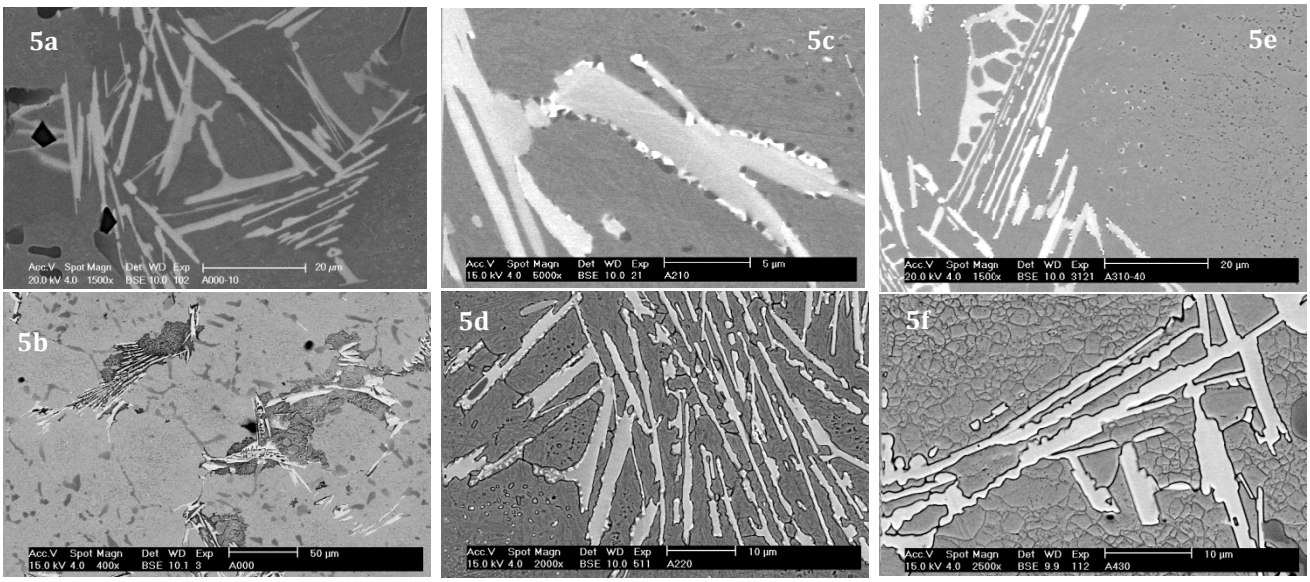

Figure 5: Evolution of M_2C eutectic carbide with various austenitizing T and time on Grade A. ***5a*** *(as-cast conditions, unetched sample – 559 HV): Untransformed M_2C at grain boundary with no secondary precipitation at the M_2C/interface;* ***5b*** *(same as 4a, Nital etched): Fine pearlite (dark etched phase) often present in the vicinity of untransformed M_2C carbides (light) – Rod-like MC (dark grey)in the interdendritic areas and a matrix composed of martensite, retained austenite and pearlite;* ***5c*** *(20' at 1025°C, unetched – 812 HV, maximum bulk hardness): Beginning of M_2C decomposition yielding secondary carbides precipitating at the M_2C/matrix interface, which are V-rich MC (dark) and Mo-rich M_6C (light) - On the same time, the remaining carbide change to a Cr-rich carbide (light grey) while keeping the shape similar to that of the previous M_2C;* ***5d*** *(60' at 1025°C, Nital etched – 748HV, minimum hardness): In situ transformation of M_2C with secondary carbides at M_2C/matrix interface;* ***5e*** *(20' at 10605°C, unetched – 793HV): M_2C carbide exhibiting some areas with the in situ phase transformation that yield secondary carbides at M_2C/matrix interface and even far away within the grain (light grey zones, Cr-rich), and others areas without any transformation of the initial M_2C (light parts of the carbide, Mo-rich);* ***5f*** *(180' at 11100°C, Nital etched – 768HV): Untransformed M_2C carbides within a surrounding matrix mostly composed of RA*

The precipitation of secondary carbides at the M_2C/matrix interface could be set as the first stage of the M_2C in situ transformation. Increasing both T or time during austenitizing strongly influence Mo-rich carbide transformation as the second stage of the transformation yield a precipitation of secondary carbides mostly in the vicinity of the grain boundaries, far away from the previous M_2C/matrix interface (fig. 5c, e). Further increases in austenitizing time yield a third stage which could be characterized by a more consistent diffusion of V and Mo escaping from the transformed M_2C carbide within the centre of the austenitic grain, while the higher austenitizing temperature could inhibit the secondary carbides precipitation as their containing elements should remain in the austenitic solid solution (fig. 5f). The matrix in the as-quenched conditions is always composed of martensite with more or less retained austenite.

Nevertheless, the in situ transformation of M_2C carbides did not systematically occur with increasing time and temperature during the austenitization on Grade A. In fact, M_2C carbides present in some areas of the quenched samples did exhibit neither a chemical modification nor a change in their morphology, as they retained both Mo and V within their elements content while no precipitates were observed within the interface (fig. 5e, f). As a reminder, the M_2C carbides present in the as-cast samples prior to heat treatment were not decomposed either (fig. 5a, b). For Grade Z, observations similar to those previously made on the Grade A could be noticed (fig. 6).

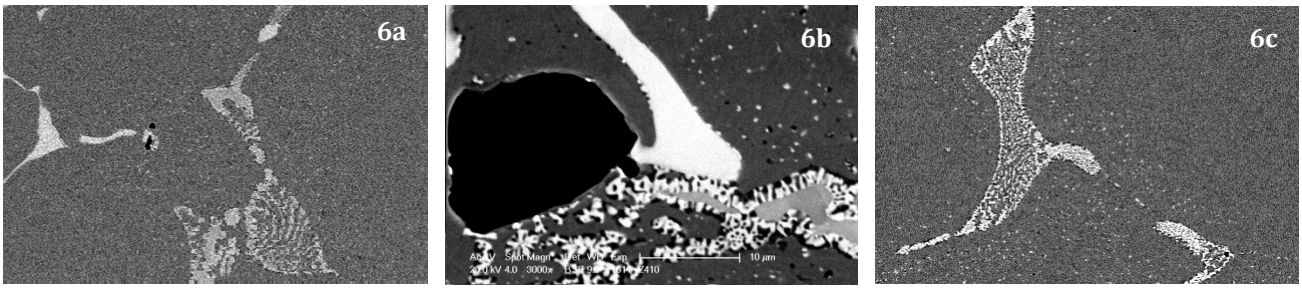

Figure 6: Evolution of M_2C eutectic carbide with various austenitizing T and t on Grade Z. ***6a*** *(20' at 1060°C; 727HV): Beginning of M_2C decomposition yielding secondary MC + M_6C carbides at M_2C/interface, with reduced amount of precipitation within the grain;* ***6b*** *(20' at 1100°C; 715HV): Maximum of the "Budding phenomenon" as the edge of the transforming M_2C is saturated with newly precipitated MC and M_6C;* ***6c*** *(180' at 1100°C;720HV): Diffusion of V and Mo that escaped from the transforming M_2C as occurred, and the precipitation of secondary MC and M_6C carbides take place within the grain, in the vicinity of the previous M_2C carbide*

Bulk hardness measurements carried out on as-quenched samples are illustrated on figure 7. For a given austenitizing temperature, the maximum of the bulk hardness is most often achieved after 60', as shorter (20') or longer (180') holding times lead to a lower hardness.

The overall maximal hardness was obtained at 1025°C for G grade (fig. 7b), and at 1060°C for both A and Z grades (fig. 7a and 7c). The average hardness together with the standard deviation (SD) could be considered in order to assess the homogeneity within the grain prior to quenching and the completion of the martensitic transformation on one hand, and the relative amount of secondary carbides precipitating inside the grain on the other hand. In fact, higher SD and low bulk hardness could be related to higher amount of retained austenite after quenching, whereas high bulk hardness with low SD suggests better completion of the martensitic transformation together with the occurrence of a large volume fraction of secondary carbides within the matrix. Thus hardness results could confirm the observations previously made on the micrographs characterization as the diffusion and the precipitation/dissolution of strong carbides forming elements within the matrix directly influence the bulk hardness in the as-quenched conditions.

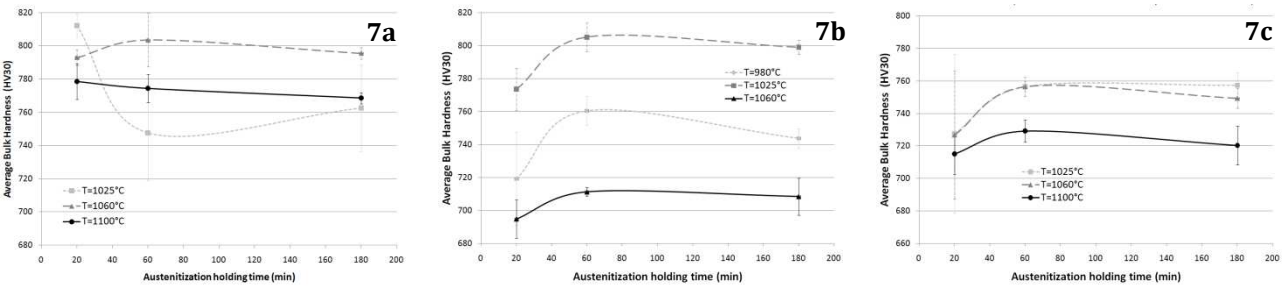

Figure 7: Bulk Hardness evolution with various austenitizing temperature and time on studied alloys. *7a: Grade A, with the maximum and minimum hardness respectively obtained after 20' at 1025°C (812HV) and after 60' at 1025°C (748HV); 7b: Grade G, with the maximum and minimum hardness respectively obtained after 60' at 1025°C (805HV) and after 20' at 1060°C (695HV); 7c: Grade Z, with three points for the maximum of the hardness (757HV), namely 1025°C/60', 1060°C/60' and 1025°C/180', and almost two points for the minimum (715HV for 1100°C/20' and 720HV for 1100°C/180')*

Quantitative metallography by image analysis

The results of image analyses performed on heat treated samples are given in figure 8 to 10. For each figure, the evolution of the average amount of carbides with thermal treatments is shown. Table 5 compares the results of the quantification based on simulations in equilibrium conditions and those obtained in as-cast conditions, especially the carbides volume fractions.

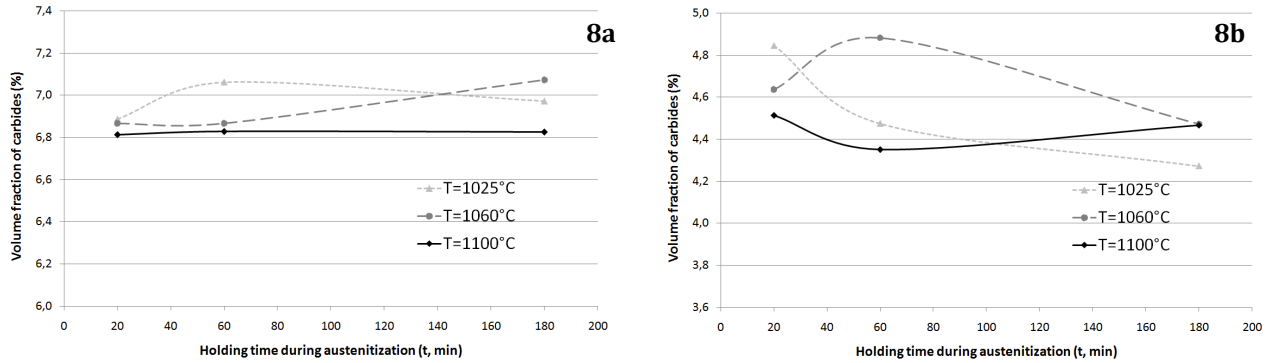

Figure 8: Evolution of MC (8a) and M_2C carbides (8b) average volume fractions with T and time on Grade A

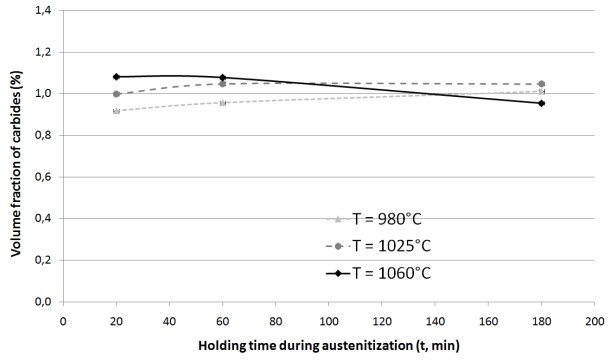

Figure 9: Evolution of M_2C carbides average volume fraction with T and time on Grade G

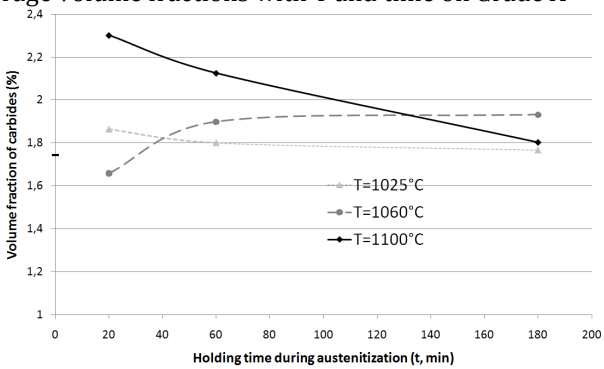

Figure 10: Evolution of the average volume fraction of MC+M_2C carbides with T and time on Grade Z

Grade A seems to contain more carbides than grade Z, as the total amount of carbides for the former is five times higher than that of the later. Heat treatments led to minor variations of the MC volume fraction in Grade A and for the M_2C volume fraction in Grade G, contrary to M_2C amount in Grade A and MC+M_2C quantity in Grade Z. Alike M_2C of Grade A, the important changes in the total carbide volume fraction with thermal treatment might be due to the Mo-rich carbide modification in Grade Z, as MC carbides a known to remain more stable.

Table 5: Comparison of carbides volume fractions (TC#As-cast conditions)

	From TC simulations (%)			
Grades	**MC**	**M_2C**	**M_7C_3**	**M_6C**
A	42	21	4	2
G	-		12	12
Z	15	3	1	5
	From Quantitative Metallography on as-cast samples (%)			
A	[6.0 -8.0]	[5.6 -5.7]		
G	-	[0.9 -1.0]	Not quantified	
Z	[1.6 -1.8]			

Discussion

Equilibrium # Non-Equilibrium

The solidification range as predicted by TC is always shorter than that obtained from DTA simulation. In fact the liquidus given by TC appears lower than the one obtained from non equilibrium simulation, whereas the TC solidus is higher than that of DTA in the same time. Contrary to the overall solidification range, the phase transformations ranges appear shorter in DTA tests than those obtained from TC simulations. Such a deviation in the transformation ranges may originate from the undercooling effect that occurs in the non equilibrium conditions and which involves segregation phenomenon that is hardly approximated in equilibrium conditions [6, 16]. Furthermore, the longer phase transformations ranges obtained from TC compared to DTA may probably be explained by the differences observed in the phase volume fractions. Indeed the volume fractions of carbides as predicted by TC are always higher than those more realistic obtained from quantitative metallography in non equilibrium conditions.

Two morphologies for M_2C carbides in the as-cast conditions

Metallographic analyses done in the as-cast conditions show no transformation of M_2C carbides in A, G and Z grades, as these carbides exhibited an homogeneous chemical composition, even if two different morphologies were found, one irregular in A grade, and the complex regular one in both G and Z alloys [6, 9]. The difference within the morphology of M_2C carbides in the as-cast conditions is probably due to the chemical composition of the studied alloys, as a similar casting route could be considered either in industrial casting or in DTA tests. In fact the acicular eutectic M_2C carbide observed on A grade precipitated around 1190°C whereas the regular M_2C carbide found in both G and Z grades had a lower eutectic temperature (below 1160°C for Z and below 1150°C for G grades). Furthermore, the occurrence of a peritectic reaction for both G and Z grades could also influence M_2C shape in the as-cast conditions as the retained liquid involved at the end of the solidification process is different from that of A grade where solidification starts with primary austenite dendrite prior to eutectic reactions leading to carbides formation [6].

Relative stability of carbides after thermal treatments

The Mo-rich M_2C carbide that often transformed itself during thermal treatment appears to be metastable for high temperature lower than its critical melting point whereas the M_6C carbide (Mo and Fe-rich), which could be obtained from the decomposition of the previous one, seems more stable. On the same time, depending on their location within the studied sample and especially the composition of the surrounding matrix, carbides similar to the metastable M_2C carbide seemed to remain untransformed while submitted to identical heat treatments in a given sample.

Thermal treatments do not seem to change the proportion of carbides, especially the MC type in both A and Z grades, and the M_7C_3 type in the G grade, even if this latter carbide was not quantified. MC and M_7C_3 carbides can therefore be considered as stable phases for the defined heat treatments performed in this work, this statement being opposite to the predictions of TC, especially for the M_7C_3 which are supposed to transform into $M_{23}C_6$ at lower temperature in equilibrium conditions.
If the stability of the MC carbides has generally been clearly established in different works [13, 25, 28], for M_7C_3 it seems to be less formal. Indeed, several studies pointed $M_{23}C_6$ as the most stable Cr-rich carbide when compared to the M_7C_3 types. Furthermore reported phase transformations of M_7C_3 into $M_{23}C_6$ or M_6C [29, 30] seem to be similar to those predicted by TC in equilibrium conditions [12, 17, 19, 22, 23]. However the apparent stability of M_7C_3 found in G grade could be related to their composition and size. Indeed, elements other than Cr, such as V and Mo that were found inside the M_7C_3 carbide could help to stabilize this carbide in a better way than Cr alone. But this apparent stability could also be due to an austenitizing temperature not higher enough compared to the critical melting point of this M_7C_3 as determined from DTA tests.
No coarsening phenomenon on MC carbides was observed with the heat treatments, as it had been previously highlighted [9, 31, 32]. The lack of coarsening for MC carbides may be explained by the fact that the matrix content in MC forming elements is low. Either V (in A grade) and Nb (in Z grade) appear to be mainly dissolved earlier in solidification carbides of MC type, with a residual V content escaping latter from M_2C decomposition to form fine secondary precipitates during heat treatments.

In situ transformation of M_2C carbides during thermal treatments

As it had been mentioned previously, no transformation of M_2C carbides was observed in the as-cast conditions. But once thermal treatments are performed, in situ transformations of some M_2C occur mainly in the 2 of the 3 studied alloys, namely A and Z grades, under some conditions that will be pointed out below.
For the mechanism of in situ M_2C transformations itself, it appears to be the same for the two morphologies of M_2C, namely regular and irregular types. Indeed, for the two types of M_2C, and for a given austenitizing temperature with increasing holding time, there was successively:

- a local decomposition of M_2C carbide which forms at the interface with the surrounding matrix, very fine V-rich MC carbides and very fine Mo-rich M_6C carbides, while leaving the previous carbide enriched in Cr;
- a diffusion of the elements containing MC and M_6C carbides away of the grain boundary and inside the grain, with a more or less related precipitation within the matrix;
- the complete dissolution of these elements for longer holding times associated with higher austenitizing temperatures.

The remaining carbide, which is Cr-rich, exhibits a shape similar to that of the originated M_2C carbide, with the outline modified at the beginning of the in situ transformation as a "budding" phenomenon related to MC and M_6C carbides precipitating at the interface M_2C/matrix was observed. "Buds" observed on the previous M_2C edge seem to depend on austenitizing time and the temperature. Moreover the evolution of the overall hardness with thermal treatments can also highlight the in situ transformation of M_2C carbide, especially the phenomenon of preferential diffusion of elements such as V and Mo that move from the

interface at grain boundary to migrate in the centre of the grain where they could precipitate later as secondary carbides [3, 5, 15]. Indeed, the precipitation of newly formed MC and M_6C secondary carbides at the M_2C/matrix interface slightly influences the overall hardness than the precipitation of the same carbides within the matrix, as a secondary hardening effect occurs in the later case. Meanwhile longer time and higher austenitizing temperature allow V, Mo and other strong carbides forming elements coming from the destabilized M_2C carbide, to remain in solid solution within the austenitic grain [3, 5, 15], thus significantly affecting the bulk hardness of the quenched samples that could collapse. Indeed an austenitic grain enriched with alloying elements and no secondary carbides precipitated can result in a coarsening of the grain followed by the lowering of the Ms point at the time of quenching, both leading to a high volume fraction of retained austenite with a low amount of martensite in the sample at room temperature [3, 5, 15]. This is probably what happened for higher austenitizing temperatures (over austenitizing) and holding time on the studied materials, as their related bulk hardness is the smallest in each case. However, the low hardness of over-austenitizing samples can be considerably increased while performing an appropriate tempering heat treatment hat will promote secondary carbide precipitation within the matrix together with the transformation of residual austenite into martensite [3, 5, 7, 15].

Regardless of the alloy grade, M_2C eutectic carbides appear to be the last phase to solidify in A, G and Z grades. Although such an analysis had not been carried out in this work, it could be assumed that the partitioning of elements in some regions of the retained liquid is not as optimized as for the phase that precipitates lately [6, 9, 16]. This assumption could then be put close to that of the previous work done on the occurrence of unexpected pearlite in the vicinity of M_2C carbides in an as-cast HSS grade similar to alloy A, as the austenite associated with M_2C carbides in order to form an eutectic colony was enriched in Cr, Mo and C. Such an austenite was considered like a degenerated M_7C_3 ready to transform later in a very fine pearlite which is enriched in Cr while containing fully dispersed Mo-rich secondary carbides at the same time [26]. This very fine pearlite is similar to an alloying elements entrapment which is mainly located in the vicinity of some M_2C carbides at the end of the casting route.

When a heat treatment is performed at a temperature above the eutectoid point, the pearlite undergoes a reverse eutectoid transformation which leads to an austenite surrounding a M_2C carbide, with a chemical composition different from that of the matrix. It should be assumed further that once alloying elements containing the transformed pearlite are dissolved in the solid solution, the local equilibrium at the interface between the newly formed austenite and the M_2C carbide is modify. Then the driving force for the beginning of the M_2C in situ transformation should be the interface diffusion of elements such as V and Mo mainly contained in the initial M_2C carbide on one hand, and C and Cr mainly contained in the previous pearlite which surrounds the initial M_2C carbide. Such an interface diffusion could be later yield to the precipitation of V-rich and Mo-rich secondary carbides directly on the edge of the transforming M2C, while Cr tend to diffuse within the previous carbide to make it transformed into a Cr-rich carbide.

As this statement is restricted to the regions where there is a previous Cr-rich fine pearlite surrounding a M_2C carbide that is known to be less stable than M_6C, the M_2C carbides which are not surrounding by such a Cr-rich matrix should not undergo the same in situ phase transformation. This is probably the case for grade G where Cr-rich pearlitic zones found in the as-cast conditions were mainly located inside the grain itself, without surrounding Mo-rich carbides. Then the diffusion of dissolved elements containing previous pearlite after austenitization may occur within the grain instead of moving to the carbide/matrix interface.

Model for M_2C in situ transformation during heat treatments

There is a preferential location for the start of M_2C in situ transformation which is the interface M_2C/matrix. This interface, which is a depleted zone, has got a chemical composition and a structure that are different from both the carbide itself and from the surrounding matrix in the grain boundary [6, 16], the later being enriched in Cr as the result of the previous location of a very fine pearlite also known as troostite [26,]. Under the temperature effect, V, Mo and probably a certain amount of Fe and C move from the centre of M_2C Carbide to the interface, where they precipitated into fine and globular MC and M_6C carbides, while Cr undergo the reverse diffusion from the neighboring matrix to the inside of the carbide. For higher austenitizing temperature and holding time, the elements that compose these newly formed secondary carbides could move from the interface to reach the centre of the grain while homogenizing the whole austenitic grain at the same time. If T and time are higher enough to keep carbide forming elements in the solid solution without precipitating as secondary carbides, then prior austenitic grain growth can occur thus leading to a higher retained austenite content after quenching [3, 5, 15].

From the previous analyses the following transformation kinetics model can be suggested for the in situ transformation of metastable M_2C carbide. This model could be broken down into fourth stages as follows (fig. 11):

- **Stage 0** (fig. 11a): Occurrence of a Cr-rich neighboring phase in the vicinity of M2C carbide such as a very fine pearlite (troostite)
- **Stage 1** (fig. 11b): Under thermal treatment, the previous troostite is transformed into a corresponding austenite where previous alloying elements containing the troostite (and possible secondary Mo-rich carbides) are dissolved
- **Stage 2** (fig. 11c): M_2C carbide destabilization under the temperature and time effect with diffusion of V, Mo, Fe and C form the centre of the carbide to the interface M_2C/matrix where V and Mo combined to C to form respectively MC and M_6C carbides that precipitate at the interface. The so-called "budding phenomenon" occurs which correspond to a slight increase in the surface fraction of the previous carbide compared to that of the as-cast conditions. The previous M_2C carbide becomes enriched with Cr to form a Cr-rich carbide (of M_7C_3 or M_3C type). The microstructure of the as-quenched samples consists in a mixed martensite and retained austenite matrix with a bulk hardness enhanced.
- **Stage 3** (for increasing T and t; fig. 11d): M_2C in situ transformation is more emphasized with a larger diffusion scale up to the center of the grain for MC and M_6C containing elements. MC and M_6C can precipitated within the grain to promote secondary hardening effect which increases the bulk hardness of the as-quenched sample compared to that of stage 1. The remaining carbide is still enriched in Cr and it keeps the same morphology as the previous M_2C carbide. The volume fraction of carbides is slightly increased compared to that of the stage 1, as secondary carbides precipitating within the grain are added to the pre-existing eutectic carbides.
- **Stage 4** (over austenitizing; fig. 11e): the higher austenitizing temperature together with the possible higher holding time help rapid diffusion of elements within the grain but in the same time, secondary carbides precipitation is reduced as carbides forming elements remain in solid solution in the austenitic grain. The previous M_2C remains enriched in Cr while keeping a shape similar to that of the initial M_2C with no secondary carbides within the interface. A possible partial dissolution of pre-existing eutectic carbides is possible, which lead to a carbide volume fraction lower than that of

the as-cast sample. The complete dissolution of carbides forming elements in the matrix with no secondary carbides leads to the possible prior austenitic grain growth and a lowering of the Ms point during quenching. The bulk hardness of the as-quenched samples collapses as the amount of retained austenite is enhanced and because the secondary hardening effect does not occur.

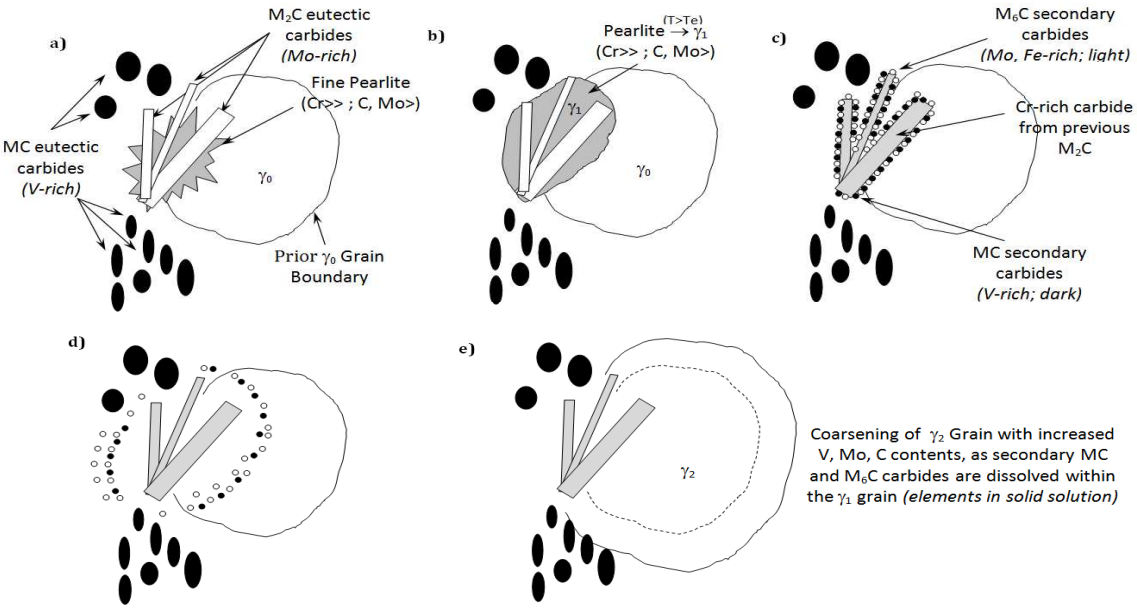

Figure 11: Sketch map of in situ transformation kinetics from M_2C eutectic carbide (+ neighboring Cr-rich matrix) to secondary MC+ M_6C carbides while leaving a Cr-rich carbide on the initial site

Conclusions

The study of 3 type HSS and semi-HSS alloys allows the comparison between equilibrium simulations and non equilibrium tests, especially the solidification range.
Carbides predicted in equilibrium conditions are quite different from those obtained after industrial casting route or DTA tests, especially Mo-rich M_2C type which is also metastable. Furthermore, the carbides volume fraction as obtained from TC is always higher than that the actual one produced form industrial casting.
The stability of M_2C carbide evaluated towards appropriate heat treatments leads to the enhancement of an in situ phase transformation with a diffusion control destabilization phenomenon.
A complete mechanism of M_2C carbides destabilization can be suggested, this mechanism being conditioned by the occurrence of a Cr-rich neighboring matrix in the vicinity of the M_2C carbide, namely a very fine pearlite such as troostite, and being promoted by austenitizing temperature and holding time.

Acknowledgments
The authors wish to thank Marichal Ketin for their deep collaboration and the supply of samples used in this study, and the Walloon Region for their support. The electron images were obtained thanks to CATμ (ULg) devices.

References

[1] A. MOLINARI, M. PELLIZZARI, A. BIGGI, G. CORBO & A. TREMEA: *Proceedings of the 6th International Tooling Conference – Karlstad, Sweden (September 2002)*, p. 437

[2] H. FU, Y. QU, J. XING, X. ZHI, Z. JIANG, M. LI & Y. ZHANG: Jrn. of Mat. Eng. and Perf., Vol. 17 n°4 (2008), p. 535

[3] Y. LUAN, N. SONG, Y. BAI, X. KANG & D. LI: Jrn. of Mat. Proc. Tech., Vol. 210 n°3 (2010), p. 536

[4] Y. MATSUBARA: *Research and Development of Abrasion Wear Resistant Cast Alloys for Rolls of Rolling and Pulverizing Mills – unknown, p. 30*

[5] J. H. LEE, J. C. OH, J. W. PARK, H. C. LEE & S. LEE: ISIJ Int., Vol. 41 n°8 (2001), p. 859

[6] M. BOCCALINI & H. GOLDENSTEIN: Int. Mat. Rev., Vol. 46 n°2 (2001), p. 92

[7] J. TCHOUFANG TCHUINDJANG & J. LECOMTE-BECKERS: Int. Jrn. of Fat., Vol. 29 n°4 (2007), p. 713

[8] C-M. LIN, C-M. CHANG, J-H. CHEN & W. WU: Jrn. of Alloys and Comp., Vol. 498 n°1 (2010), p. 30

[9] M. DURAND-CHARRE: *La microstructure des aciers et des fontes. Genèse et interprétation* – SIRPE Ed (Sept 2003)

[10] A. LESKO & E. NAVARA: Mat. Char., Vol. 36 n°4-5 (1996), p. 349

[11] E. FRAS, M. KAWALEC & H.F. LOPEZ: Mat. Sci. and Eng. A, Vol. 524 n°1-2 (2009), p. 193

[12] P. DING, G. SHI & S. ZHOU: Met. and Mat. Trans., A Vol. 24 n°6 (1993), p. 1265

[13] M. HASHIMOTO, O. KUBO & Y. MATSUBARA: ISIJ Int., Vol. 44 n°2 (2004), p. 372

[14] J. D. B. De MELLO, S. HAMAR-THIBAULT & M. DURAND-CHARRE: Jrn. of Mat. Sci., Vol. 20 n°10 (1985), p. 3453

[15] P. MICHAUD, D. DELAGNES, P. LAMESLE, M. H. MATHON & C. LEVAILLANT: Acta Mater., Vol. 55 n°14 (2007), p. 4877

[16] T. OKANE & T UMEDA: Sci. and Tech. of Adv. Mat., Vol. 2 n°1 (2001), p. 247

[17] E-S. LEE, W-J. PARK, J. Y. JUNG & S. AHN: Met. and Mat. Trans. A, Vol. 29 n°5 (1998), p. 1395

[18] X. ZHANG: Mat. Sci. and Eng. A, Vol. 247 n°1-2 (1998), p. 214

[19] L. BOURITHIS & G. D. PAPADIMITRIOU: Mat. Sci. and Eng. A, Vol. 361 n°1-2 (2003), p. 165

[20] J. T. H. PEARCE & D. W. L. ELWELL: Jrn. of Mat. Sci. Let., Vol. 5 n°10 (1986), p. 1063

[21] A. INOUE, S. ARAKAWA & T. MASUMOTO: Trans. JIM Vol. 19 n°1 (1978), p. 11

[22] S. KARAGOZ, I. LIEM, E. BISCHOFF & H. F. FISCHMEISTER: Met. and Mat. Trans. A, Vol. 20 n°12 (1989), p. 2695

[23] A. WIENGMOON, T. CHAIRUANGSRI & J. T. H. PEARCE: ISIJ Int., Vol. 44 n°2 (2004), p. 396

[24] H. DJEBAILI, H. ZEDIRA, A. DJELLOUL & A. BOUMAZA: Mat. Char., Vol. 60 n°9 (2009), p. 946

[25] R. S. IRANI, C. S. WRIGHT & A. S. WRONSKI: Jrn. of Mat. Sci. Let., Vol. 1 n°7 (1982), p. 318

[26] J. TCHOUFANG TCHUINDJANG & J. LECOMTE-BECKERS : Sol. State Phen., Vol. 172-174 (2011), p. 803

[27] http://rsbweb.nih.gov/ij/plugins/multi-thresholder.html, see online on June 15th 2011

[28] R. PIOTRKOWSKI & R. A. VERSACI: Jrn. of Mat. Sci. Let., Vol. 6 n°12 (1987), p. 1382

[29] A. D. B. GINGELL, H. K. D. H. BHADESHIA, D. G. JONES & K. J. A. MAWELLA: Jrn. of Mat. Sci., Vol. 32 n°18 (1997), p. 4815

[30] A. INOUE & T. MASUMOTO: Met. and Mat. Trans. A, Vol. 11 n°5 (1980), p. 739

[31] X. HU, L. LI a M. ZHANG: Int. Jrn. of Fat., Vol. 28 n°3 (2006), p. 175

[32] T. NYKIEL & T. HRYNIEWICZ: Met. and Mat. Trans. A, Vol. 31 n°10 (2000), p. 2661